Effect of the computational domain on direct simulations of turbulent channels up to $Re_\tau = 4200$

Adrián Lozano-Durán, and Javier Jiménez

Citation: Physics of Fluids **26**, 011702 (2014);
View online: https://doi.org/10.1063/1.4862918
View Table of Contents: http://aip.scitation.org/toc/phf/26/1
Published by the American Institute of Physics

PHYSICS OF FLUIDS **26**, 011702 (2014)

Effect of the computational domain on direct simulations of turbulent channels up to $Re_\tau = 4200$

Adrián Lozano-Durán[a] and Javier Jiménez
School of Aeronautics, U. Politécnica de Madrid, 28040 Madrid, Spain

(Received 28 October 2013; accepted 9 January 2014; published online 22 January 2014)

The effect of domain size on direct numerical simulations of turbulent channels with periodic boundary conditions is studied. New simulations are presented up to $Re_\tau = 4179$ in boxes with streamwise and spanwise sizes of $2\pi h \times \pi h$, where h is the channel half-height. It is found that this domain is large enough to reproduce the one-point statistics of larger boxes. A simulation in a box of size $60\pi h \times 6\pi h$ is used to show that a contour of the two-dimensional premultiplied spectrum of the streamwise velocity containing 80% of the kinetic energy closes at $\lambda_x \approx 100h$. © *2014 AIP Publishing LLC*. [http://dx.doi.org/10.1063/1.4862918]

It is unclear how large the computational domain has to be in direct numerical simulations (DNS) of plane turbulent channels to avoid unphysical constraints on the largest flow scales. Previous work has determined the minimal boxes for "healthy" turbulence in the buffer region[1] and in the logarithmic layer,[2] in the sense of providing correct one-point statistics. Those results suggest that the whole flow would be healthy for boxes wider than about $3h$, where h is the channel half-height.[2] However, even in the largest domains simulated until now, the premultiplied spectrum of the streamwise velocity remains unclosed for a contour of 20% of its maximum,[3] which only contains about 70% of the total energy. Moreover, some of the longest ejections in those boxes span the full length of the simulation domain,[4] even though they carry a substantial fraction of the total Reynolds stress.[4,5] In both cases, the longest structures are presumably misrepresented. Their maximum length remains unknown, and so are the consequences of constraining them. Our goal is to examine the effect of the domain size on the large-scale structures of the flow, as well as on the velocity and pressure statistics, and to determine the smallest box that reproduces across the full channel height one-point statistics identical to those in the larger domains. Smaller-scale quantities such as the vorticities are not expected to be influenced by the box size.

We have performed five new DNSs of plane turbulent channels. Their parameters are summarized in Table I together with the older simulations used for comparison. In all of them, the incompressible flow is integrated in the form of evolution equations for the wall-normal vorticity and for the Laplacian of the wall-normal velocity,[6] and the spatial discretization is dealiased Fourier in the two wall-parallel directions. Cases with $Re_\tau < 1000$ use Chebychev polynomials in y, while those with $Re_\tau \geq 2000$ use seven-point compact finite differences.[7] Time stepping is third-order semi-implicit Runge-Kutta[8] with CFL = 0.5. The streamwise, wall-normal and spanwise coordinates are x, y, and z, respectively, and the mean streamwise velocity is $U(y)$. The corresponding components of the velocity fluctuations with respect to the mean are u, v, and w. Primed quantities are root-mean-squared intensities, and the superscript $+$ denotes wall units based on the friction velocity u_τ and on the kinematic viscosity ν. The Kármán number is $Re_\tau = h^+$.

The very small case VS950 is a minimal box for the logarithmic layer from Ref. 9, and is known to have incorrect statistics above $y \approx L_z/3 \approx 0.25h$.[2] The new small case S950 has a somewhat larger computational domain with streamwise and spanwise periodicities $L_x = \pi h$ and $L_z = \pi h/2$ at $Re_\tau = 939$, and Ref. 2 suggests that its statistics should fail above $y \approx 0.5h$. The medium cases M950,

[a]adrian@torroja.dmt.upm.es

TABLE I. Parameters of the simulations. $Re_\tau = h^+$ is the Kármán number. L_x and L_z are the streamwise and spanwise dimensions of the numerical box and h is the channel half-height. Δx and Δz are the spatial resolutions in terms of Fourier modes before dealiasing. Δy_{max} is the coarser spatial resolution in the wall-normal direction. N_y is the number of wall-normal collocation points. Tu_τ/h is the total time used for statistics after discarding transients, in eddy turnovers. The initial letter of each case is related with the size of the domain: very small (VS), small (S), medium (M), large (L), and very large (VL). The entries starting with (E) are experimental channels.[12]

Case	Re_τ	L_x/h	L_z/h	Δx^+	Δz^+	Δy^+_{max}	N_y	Tu_τ/h	Lines and symbols
VS950[9]	948	$\pi/2$	$\pi/4$	11.6	5.8	7.8	769	77	– – – (black)
S950 (present)	938	π	$\pi/2$	11.5	5.8	7.7	385	110	– · – · – (magenta)
M950 (present)	932	2π	π	11.5	5.7	7.7	385	20	– ● – (magenta)
M2000 (present)	2009	2π	π	12.3	6.2	8.9	633	11	– ■ – (blue)
M4200 (present)	4179	2π	π	12.8	6.4	10.7	1081	15	——— (red)
L550[10]	547	8π	4π	13.4	6.8	6.7	257	22	– ▲ – (green)
L950[11]	934	8π	3π	11.5	5.7	7.6	385	12	– ○ – (black)
L2000[3]	2003	8π	3π	12.3	6.1	8.9	633	11	– □ – (black)
VL550 (present)	547	60π	6π	12.6	5.0	6.7	257	5	– △ – (black)
E1000[12]	1010	...	...	...	...	...	...	...	+ (magenta)
E2000[12]	1960	...	...	...	...	...	...	...	* (blue)
E4000[12]	4050	...	...	...	...	...	...	...	◊ (red)

M2000, and M4200 have boxes with $L_x = 2\pi h$ and $L_z = \pi h$, with $Re_\tau = 932$, 2009, and 4179, respectively. The older large cases L550,[10] L950,[11] and L2000[11] have domains with $L_x = 8\pi h$ and $L_z \geq 3\pi h$, while the new very large case VL550 has a box size $L_x = 60\pi h$ and $L_z = 6\pi h$, and is intended to test whether there is a largest size for the structures that develop in the channel. The lines and symbols in Table I are used consistently in later plots, and are chosen so that DNSs with the same Re_τ have similar symbols, unless otherwise stated. We also include results from the experimental channels by Schultz and Flack[12] at $Re_\tau = 1010 - 4050$, denoted by E1000 to E4000. They are plotted in the same color as the DNS with the closest Re_τ. The case with the highest Reynolds number is the new M4200, with $Re_\tau = 4179$. It reaches a maximum Taylor-microscale Reynolds number $Re_\lambda = q^2[5/(3\nu\epsilon)]^{1/2} \approx 200$, at $y \approx 0.4h$, where $q^2 = u^2 + v^2 + w^2$ is the magnitude of the velocity fluctuations and ϵ is the kinetic-energy dissipation rate. Assuming that the smallest coherent structures are of order 10η,[13] where $\eta = (\nu^3/\epsilon)^{1/4}$ is the Kolmogorov viscous length, the resulting scale separation is $h/10\eta \approx 100$.

The mean streamwise velocity profiles are shown in Fig. 1(a). They collapse reasonably well to a common logarithmic behavior for all the Reynolds numbers, experiments, simulations, and box

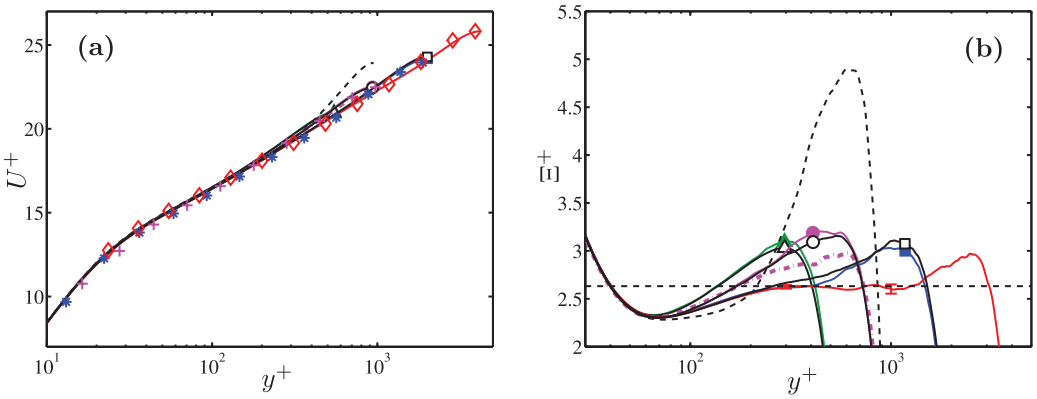

FIG. 1. (a) Mean streamwise velocity profiles. (b) Logarithmic-law diagnostic functions. The dashed horizontal line corresponds to a Kármán constant $\kappa = 0.38$. Lines and symbols are as in Table I.

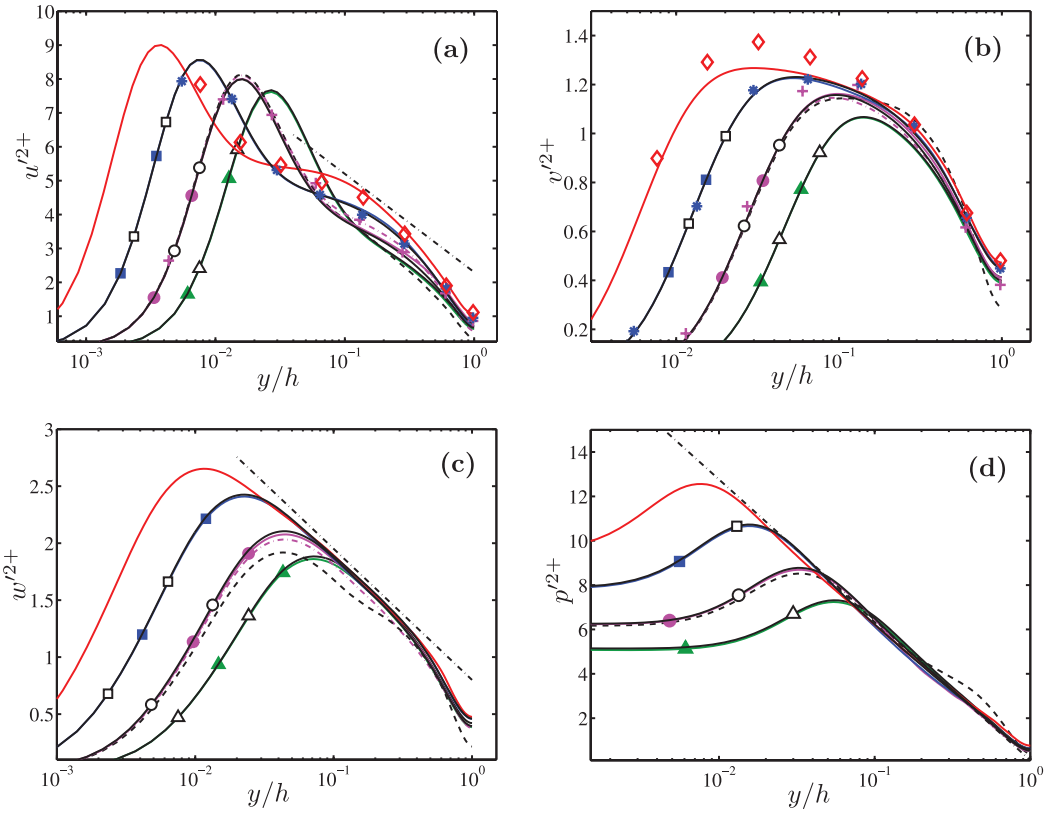

FIG. 2. (a)-(c) Streamwise, wall-normal, and spanwise mean-squared velocity fluctuations. (d) Mean-squared pressure fluctuations. The dashed-dotted line in (a) is $u'^2 = 2.25 - 1.26\log(y/h)$ from Ref. 26, the one in (c) $w'^2 = 0.80 - 0.50\log(y/h)$ from Ref. 21, and the one in (d) $p'^2 = 0.10 - 2.75\log(y/h)$ from Ref. 23. Other lines and symbols are as in Table I.

sizes. The only anomalous behavior is the bump in the core of the smallest box (VS950), which is accelerated with respect to the other cases. To test the logarithmic behavior in more detail, Fig. 1(b) shows the diagnostic function

$$\Xi^+ = y^+ \partial U^+ / \partial y^+, \tag{1}$$

which is equal to the inverse of the Kármán constant κ wherever the mean profile is logarithmic. The only case with an incipient logarithmic layer is M4200, for which $\kappa \approx 0.38$ is within the scatter of the values obtained by other authors.[14–17] The agreement between the large (L950, L2000) and medium (M950, M2000) boxes is excellent across the whole channel, especially when compared with the differences with the smaller boxes, S950 and VS950. As expected, $U(y)$ and Ξ are identical for the large and very-large cases L550 and VL550. Experiments are not included in the diagnostic plot because of the relatively large scatter of the derivatives of their velocity profiles. Note that one-standard-deviation error bar has been added to Fig. 1(b) for case M4200 at $y^+ = 1000$, computed as in the appendix of Ref. 18. The error bars for other simulations are of the order of the thickness of the lines used to plot statistics, and are omitted. For cases L2000 and M2000 whose statistics have been accumulated for the same amount of eddy turnovers, the errors in u' at the center of the channel are roughly 3.4 times smaller in the large box. If we suppose that each snapshot from case L2000 is equivalent to $8\pi \times 3\pi/(2\pi \times \pi) = 12$ snapshots from case M2000, the result agrees well with the theoretical[18] value $\sqrt{12} \approx 3.5$ and the statistical uncertainties decrease inversely proportional to the square-root area of the box simulated.

The mean-squared velocity and pressure fluctuations are presented in Figs. 2(a) and 2(d). We briefly highlight some aspects regarding the effect of the box size and of the Reynolds number, and the reader is referred to Refs. 3 and 19–23 for a more detailed physical discussion. The profiles of

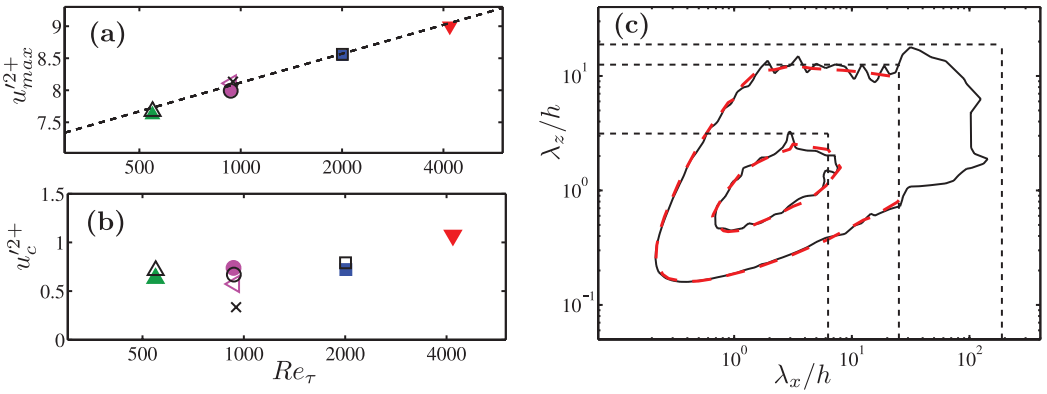

FIG. 3. (a) Maximum of the mean-squared streamwise velocity fluctuations, u'^2_{max}. The dashed line is $u'^{2+}_{max} = 3.63 + 0.65\log(Re_\tau)$ from Ref. 23. (b) Mean-squared streamwise velocity fluctuations, u'^2_c, at the center of the channel ($y = h$). Symbols are as in Table I except for: ▼ (red), M4200; × (black) VS950; and ◁ (magenta), S950. (c) Premultiplied two-dimensional spectra of the streamwise velocity, ϕ_{uu}, at $y = h$, as a function of the streamwise and spanwise wavelengths. The contours are 0.1 and 0.6 of the maximum value of ϕ_{uu}. (– – –) (red), case L550; (———), case VL550. The dashed lines mark the box dimensions, L_x and L_z, for the medium, large, and very large domains.

the mean-squared spanwise velocity fluctuations w'^2 are logarithmic, as predicted in Ref. 24, and as already reported in Refs. 21, 23, and 25. This becomes more evident as the Reynolds number increases. The same is not true of the streamwise velocity fluctuations u'^2, for which a logarithmic region cannot be found even at the highest simulated Reynolds number. The profile of u'^2 gets flatter with Re_τ in the inner part of the region where the logarithmic behavior appears for the other variables,[23,26] and it is unclear from the present data whether it will develop a local maximum, a plateau, or an actual logarithmic region for higher Reynolds numbers. Experiments in pipes[26] suggest that u'^2 also develops a logarithmic range, although probably only in the outer part of the overlap layer. The asymptotic empirical law given in that paper has been added to Fig. 2(a), and is tangent to M4200 and to E4000. An experimental channel at $Re_\tau \approx 6000$,[12] not included in the figure, approximately follows that logarithmic behavior over a narrow range, suggesting that simulations at moderately higher Reynolds numbers than the present ones should begin to show it. The mean-squared wall-normal velocity fluctuations v'^2 do not have a logarithmic range, as expected from the constraints imposed by impermeability.[19] Experimental and DNS data are in reasonable agreement, although v'^2 is slightly higher in E4000 than in the comparable simulation. Fluctuations for large (L950, L2000) and medium (M950, M2000) simulations agree very well at all heights, including the growth with Re_τ of u'^2 at its near-wall maximum (Fig. 3(a)), and at the center of the channel (Fig. 3(b)). Even the pressure fluctuations, which could be expected to be more sensitive than the velocities to the global effects of the box size, agree well between large and medium boxes. These results support the prediction in Ref. 2 that the $L_z \approx \pi$ is sufficient to obtain good statistics up to the center of the channel. It is also reassuring that there are no differences between the statistics of cases L550 and VL550, supporting the conclusion that the simulation boxes used at present are large enough to capture the one-point statistics of all the flow variables. The small box S950 has only minor differences in the mean-squared fluctuations with respect to the medium boxes, although we have seen that the logarithmic-law diagnostic function is more sensitive. On the other hand, the smaller box VS950 shows important deviations for the three velocity fluctuations above $y/h \approx 0.25$.[2]

It was already noted by del Álamo *et al.*[11] that the resolved part of the velocity spectrum is not strongly affected by the size of the domain. The same is found to be true when comparing the spectral densities of the present medium and large boxes (not shown). Essentially, the spectra in the medium boxes follow those in the large ones until they are truncated at the maximum wavelengths fitting in the domain. A comparison between the premultiplied spectra, ϕ_{uu}, of the large and very large boxes, L550 and VL550, is presented in Fig. 3(c). The lowest contour plotted is 10% of the maximum of ϕ_{uu} and contains roughly 80% of the streamwise kinetic energy. The spectrum of L550 is truncated by the box, but that of VL550 is not. Very large structures of length $O(25h)$ have been

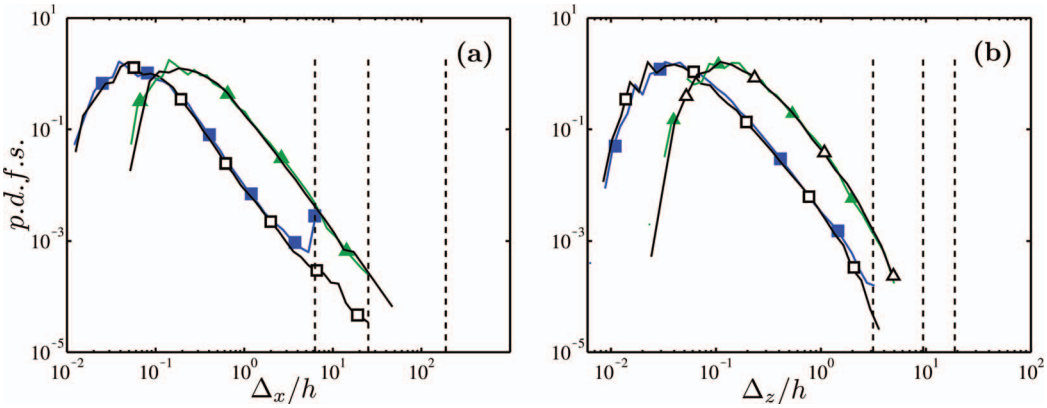

FIG. 4. Probability density functions of the logarithm of the size of the coherent uv-structures. (a) Streamwise size, Δ_x. (b) Spanwise size, Δ_z. The vertical dashed lines are the edges of the domain for medium, large, and very large boxes. Lines and symbols are as in Table I.

documented before in pipes and channels,[5,11,27–31] but, to our knowledge, this is the first time that such a low energy contour has been shown to close within the computational box or within the spatial experimental domain. That result sets a new lower limit of $\lambda_x \approx 100h$ for the wavelengths at which some of the energy of the streamwise velocity fluctuations can be found.

In the last part of this paper, we focus on the effect of the size of the domain on the coherent structures studied in Lozano-Durán, Flores, and Jiménez.[4] Briefly, they are the structures contributing most to the tangential Reynolds stress, and are obtained by extending the one-dimensional quadrant analysis of Lu and Willmarth[32] to three dimensions. The structures are defined as connected regions satisfying

$$|\tau(\boldsymbol{x})| > Hu'(y)v'(y), \tag{2}$$

where $\tau(\boldsymbol{x}) = -u(\boldsymbol{x})v(\boldsymbol{x})$ is the instantaneous point-wise tangential Reynolds stress and the threshold $H = 1.75$ is chosen from a percolation analysis detailed in Ref. 4. All the points satisfying (2) are classified into individual objects connected along any of the six orthogonal directions in the Cartesian grid of the DNS. Following previous works,[4,33] the sizes of the structures are measured by circumscribing them within boxes aligned to the Cartesian axes, whose streamwise and spanwise sizes are respectively denoted by Δ_x and Δ_z. We are interested in studying the effect on those sizes of confining the structures in medium, large, and very large boxes. Figures 4(a) and 4(b) show the probability density functions (pdfs) of the logarithms of Δ_x and Δ_z. The distribution of spanwise sizes is barely affected by the size of the domain. On the contrary, the largest structures in x are found for case VL550, with streamwise lengths of the order of $40h$. They probably correspond to the very large-scale motions reported in Refs. 5, 11, and 27–30. They are somewhat shorter than the u-structures implied by the spectra in Fig. 3(c), in agreement with previous observations that the Reynolds-stress cospectrum is shorter than ϕ_{uu}.[11,21] The distribution of streamwise sizes in the medium box only differs from that in the larger domain at the limit $\Delta_x \approx L_x$, where it develops a peak caused by the accumulation of structures that would otherwise be longer than L_x, but do not fit in the domain. In agreement with that interpretation, the total probability contained in that peak is roughly the same as the one in the tail of the longer pdf. The number of structures per unit area with $\Delta_x \geq 2\pi h$ is $(0.041h^{-2})$ for M2000 and $(0.039h^{-2})$ for L2000. It is important to realize that because of the periodic boundary condition, these structures are seen by the flow in the shorter box as being infinitely long. The good agreement of the one-point statistics for large and medium boxes in Figs. 2(a) and 2(d) suggests that these infinitely long structures capture most of the dynamics of the actual ones, or at least of their interactions with the smaller scales of size $O(h)$. This is reasonable

considering the disparity of lengths and times scales between them and the rest of the scales in the flow. A similar argument applies to the truncated spectral density of the streamwise velocity.[11]

In summary, five new DNSs of plane turbulent channels have been presented. Three of them are computed in moderate domains with streamwise and spanwise sizes of $L_x = 2\pi h$ and $L_z = \pi h$ at $Re_\tau = 932$, 2009, and 4179. The two lowest Reynolds numbers, for which similar simulations exist in boxes with $L_x = 8\pi h$ and $L_z = 3\pi h$, have identical one-point statistics to the larger simulations, giving some confidence that the smaller boxes can be used for simulations with this particular purpose. This is true even if the largest structures are found not to fit within the smaller simulation box, as shown by the spectrum of the streamwise velocity, and by the pdfs of the streamwise length of the structures responsible for the momentum transfer.[4] It is argued that, because of the periodic boundary condition, these very large structures are essentially infinitely long in the smaller boxes, but that their interaction with the well-resolved scales is correctly represented. Note that these medium-sized boxes are not necessarily cheaper to simulate than larger ones, because they have to run for longer times to accumulate comparable statistics, but they can typically be run in smaller computers. In contrast, the statistics of even smaller boxes, with $L_z \leq \pi/2$ differ significantly from the larger simulations, as predicted in Ref. 2, with the largest discrepancies affecting the mean velocity profile.

The simulation with the highest Reynolds number, $Re_\tau = 4179$, continues the trends of the previously available simulations at lower Re_τ. For example, it confirms the growth with Re_τ of the near-wall peak of the mean-squared streamwise velocity fluctuations. It also shows an incipient logarithmic region in the diagnostic function of the mean velocity profile, with a Kármán constant $\kappa \approx 0.38$. No logarithmic range is found for u'^2, in contrast with clear ones for w'^2 and p'^2. Finally, in order to further test the effect of relaxing the constrains to the flow due to the limited numerical domain, a new simulation was performed in a very large box with $L_x = 60\pi h$ and $L_z = 6\pi h$ at $Re_\tau = 547$. No change was found in the one-point statistics, but the two-dimensional premultiplied spectrum of the streamwise velocity was shown to close for wavelengths of the order of $\lambda_x \approx 100h$ at the level of the contour containing 80% of the streamwise kinetic energy.

This work was supported in part by CICYT under Grant No. TRA2009-11498, and by the European Research Council under Grant No. ERC-2010.AdG-20100224. A. Lozano–Durán was supported by an FPI fellowship from the Spanish Ministry of Education and Science. The computations were made possible by generous grants of computer time from CeSViMa (Centro de Supercomputación y Visualización de Madrid) and from the Barcelona Supercomputing Center. We are deeply grateful to J. A. Sillero for his careful revision of the paper, and to M. P. Schultz and K. A. Flack for providing electronic copies of their data.

[1] J. Jiménez and P. Moin, "The minimal flow unit in near-wall turbulence," J. Fluid Mech. **225**, 213–240 (1991).
[2] O. Flores and J. Jiménez, "Hierarchy of minimal flow units in the logarithmic layer," Phys. Fluids **22**, 071704 (2010).
[3] S. Hoyas and J. Jiménez, "Scaling of the velocity fluctuations in turbulent channels up to $Re_\tau = 2003$," Phys. Fluids **18**, 011702 (2006).
[4] A. Lozano-Durán, O. Flores, and J. Jiménez, "The three-dimensional structure of momentum transfer in turbulent channels," J. Fluid Mech. **694**, 100–130 (2012).
[5] M. Guala, S. E. Hommema, and R. J. Adrian, "Large-scale and very-large-scale motions in turbulent pipe flow," J. Fluid Mech. **554**, 521–542 (2006).
[6] J. Kim, P. Moin, and R. D. Moser, "Turbulence statistics in fully developed channel flow at low Reynolds number," J. Fluid Mech. **177**, 133–166 (1987).
[7] S. K. Lele, "Compact finite difference schemes with spectral-like resolution," J. Comput. Phys. **103**, 16–42 (1992).
[8] P. R. Spalart, R. D. Moser, and M. M. Rogers, "Spectral methods for the Navier-Stokes equations with one infinite and two periodic directions," J. Comput. Phys. **96**, 297–324 (1991).
[9] J. Jiménez, "How linear is wall-bounded turbulence?" Phys. Fluids **25**, 110814 (2013).
[10] J. C. del Álamo and J. Jiménez, "Spectra of the very large anisotropic scales in turbulent channels," Phys. Fluids **15**, L41–L44 (2003).
[11] J. C. del Álamo, J. Jiménez, P. Zandonade, and R. D. Moser, "Scaling of the energy spectra of turbulent channels," J. Fluid Mech. **500**, 135–144 (2004).
[12] M. P. Schultz and K. A. Flack, "Reynolds-number scaling of turbulent channel flow," Phys. Fluids **25**, 025104 (2013).
[13] J. Jiménez, A. A. Wray, P. G. Saffman, and R. S. Rogallo, "The structure of intense vorticity in isotropic turbulence," J. Fluid Mech. **255**, 65–90 (1993).
[14] J. C. Klewicki, "Reynolds number dependence, scaling, and dynamics of turbulent boundary layers," J. Fluids Eng. **132**, 094001 (2010).

[15] I. Marusic, B. J. McKeon, P. A. Monkewitz, H. M. Nagib, A. J. Smits, and K. R. Sreenivasan, "Wall-bounded turbulent flows at high Reynolds numbers: Recent advances and key issues," Phys. Fluids **22**, 065103 (2010).
[16] A. J. Smits, B. J. McKeon, and I. Marusic, "High-Reynolds number wall turbulence," Annu. Rev. Fluid Mech. **43**, 353–375 (2011).
[17] J. Jiménez, "Cascades in wall-bounded turbulence," Annu. Rev. Fluid Mech. **44**, 27–45 (2012).
[18] S. Hoyas and J. Jiménez, "Reynolds number effects on the Reynolds-stress budgets in turbulent channels," Phys. Fluids **20**, 101511 (2008).
[19] A. A. Townsend, *The Structure of Turbulent Shear Flows*, 2nd ed. (Cambridge University Press, Cambridge, 1976).
[20] M. M. Metzger and J. C. Klewicki, "A comparative study of near-wall turbulence in high and low Reynolds number boundary layers," Phys. Fluids **13**, 692–701 (2001).
[21] J. Jiménez and S. Hoyas, "Turbulent fluctuations above the buffer layer of wall-bounded flows," J. Fluid Mech. **611**, 215–236 (2008).
[22] M. Hultmark, M. Vallikivi, S. C. C. Bailey, and A. J. Smits, "Turbulent pipe flow at extreme Reynolds numbers," Phys. Rev. Lett. **108**, 094501 (2012).
[23] J. A. Sillero, J. Jiménez, and R. D. Moser, "One-point statistics for turbulent wall-bounded flows at Reynolds numbers up to $\delta^+ \approx 2000$," Phys. Fluids **25**, 105102 (2013).
[24] A. A. Townsend, "Equilibrium layers and wall turbulence," J. Fluid Mech. **11**, 97–120 (1961).
[25] J. Jiménez, S. Hoyas, M. P. Simens, and Y. Mizuno, "Turbulent boundary layers and channels at moderate Reynolds numbers," J. Fluid Mech. **657**, 335–360 (2010).
[26] I. Marusic, J. P. Monty, M. Hultmark, and A. J. Smits, "On the logarithmic region in wall turbulence," J. Fluid Mech. **716**, R3 (2013).
[27] J. Jiménez, "The largest scales of turbulence," in *CTR Annual Research Briefs* (Stanford University, 1998), pp. 137–154.
[28] K. Kim and R. J. Adrian, "Very large-scale motion in the outer layer," Phys. Fluids **11**, 417–422 (1999).
[29] I. Marusic, "On the role of large-scale structures in wall turbulence," Phys. Fluids **13**, 735–743 (2001).
[30] J. Jiménez, J. C. Del Álamo, and O. Flores, "The large-scale dynamics of near-wall turbulence," J. Fluid Mech. **505**, 179–199 (2004).
[31] J. P. Monty, J. A. Stewart, R. C. Williams, and M. S. Chong, "Large-scale features in turbulent pipe and channel flows," J. Fluid Mech. **589**, 147–156 (2007).
[32] S. S. Lu and W. W. Willmarth, "Measurements of the structure of the Reynolds stress in a turbulent boundary layer," J. Fluid Mech. **60**, 481–511 (1973).
[33] J. C. del Álamo, J. Jiménez, P. Zandonade, and R. D. Moser, "Self-similar vortex clusters in the turbulent logarithmic region," J. Fluid Mech. **561**, 329–358 (2006).